

The hadronic vacuum polarization function with $O(a)$ -improved Wilson fermions - an update

MITP/16-004

Michele Della Morte¹, Gregorio Herdoiza⁴, Hanno Horch^{*3}, Benjamin Jäger⁵, Harvey Meyer³, Hartmut Wittig^{2,3}

¹ CP3-Origins & Danish IAS, University of Southern Denmark
Campusvej 55, DK-5230 Odense M, Denmark and IFIC (CSIC)
Calle Catedrático José Beltrán, 2. E-46980, Paterna, Spain

² Helmholtz Institute Mainz, Johannes Gutenberg Universität Mainz, 55099 Mainz, Germany

³ PRISMA Cluster of Excellence, Institut für Kernphysik, Johannes Gutenberg Universität Mainz,
55099 Mainz, Germany

⁴ Instituto de Física Teórica UAM/CSIC and Departamento de Física Teórica,
Universidad Autónoma de Madrid, Cantoblanco, E-28049 Madrid, Spain

⁵ Department of Physics, College of Science, Swansea University, SA2 8PP, Swansea, UK

E-mail: horch@kph.uni-mainz.de, dellamor@cp3-origins.net
gregorio.herdoiza@uam.es, B.Jaeger@swansea.ac.uk,
meyerh@kph.uni-mainz.de, wittig@kph.uni-mainz.de

We present an update of our lattice QCD study of the vacuum polarization function using $O(a)$ -improved $N_f = 2$ Wilson fermions with increased statistics and a large set of momenta. The resulting points are highly correlated and thus require a correlated fitting procedure. We employ an extended frequentist method to estimate the systematic uncertainties due to the momentum dependence and to the continuum and chiral extrapolations. We present preliminary results of the leading order hadronic contribution of the anomalous magnetic moment of the muon (a_μ^{HLO}) at the physical point for u, d, s and c valence quarks.

The 33rd International Symposium on Lattice Field Theory
14 -18 July 2015
Kobe International Conference Center, Kobe, Japan*

*Speaker.

1. Introduction

The anomalous magnetic moment of the muon is one of the most precisely measured quantities in physics. However, for a number of years there has been a persistent $\sim 3.5 \sigma$ discrepancy between experimental measurements and the prediction from theory [1],

$$\begin{aligned} a_\mu^{exp} &= 116592091(54)(33) \cdot 10^{-11}, \\ a_\mu^{th} &= 116591803(01)(42)(26) \cdot 10^{-11}. \end{aligned}$$

The theoretical error is dominated by hadronic contributions. The lowest-order hadronic contribution is estimated using a dispersion relation relying on experimental data, so a determination from first principles using lattice QCD is desirable. This has led to interest in the lattice community and several groups have reported results [2–5]. For the determination of the hadronic vacuum polarization (HVP) tensor on the lattice we use

$$\Pi_{\mu\nu}(Q) = Z_V \sum_x e^{iQx} \left\langle J_\mu^{(c)}(x) J_\nu^{(l)}(0) \right\rangle, \quad (1.1)$$

where $J_\mu^{(c)}(x)$, and $J_\nu^{(l)}(x)$ refer to conserved and local vector currents, respectively, and Z_V is the renormalization factor of the local current [6]. The HVP is then given by

$$\Pi_{\mu\nu}(Q) = (Q_\mu Q_\nu - \delta_{\mu\nu} Q^2) \Pi(Q^2). \quad (1.2)$$

To determine a_μ^{HLO} the renormalized HVP, $\hat{\Pi}(Q^2) = 4\pi^2(\Pi(Q^2) - \Pi(0))$, is inserted into the convolution integral [7, 8]

$$a_\mu^{\text{HLO}} = \left(\frac{\alpha}{\pi}\right)^2 \int_0^\infty \frac{dQ^2}{Q^2} w(Q^2/m_\mu^2) \hat{\Pi}(Q^2), \quad (1.3)$$

$$w(r) = 16 / \left(r^2 \left(1 + \sqrt{1 + 4/r} \right)^4 \sqrt{1 + 4/r} \right), \quad (1.4)$$

where the integrand in eq. (1.3) is dominated by the region around $Q^2 \sim m_\mu^2$.

2. Lattice setup and the extended frequentist method

We use $O(a)$ -improved Wilson fermions with two dynamical degenerate light quarks and partially quenched strange and charm quarks. We use the ensembles generated within the CLS effort listed in table 1. Twisted boundary conditions are applied to increase the number of available momenta and to gain access to small momenta [9–11].

The data are highly correlated among the Q^2 momenta, and the large number of data points often lead to singular correlated covariance matrices. To avoid singularities, we randomly select subsets of 30 and 40 points in the interval $0 < Q^2 < 4 \text{ GeV}^2$. The data points at larger Q^2 values are very precise but only represent a small contribution to the convolution integral in eq. (1.3), so that we focus on data points in low Q^2 regime. In order to determine the number of samples chosen, we compute the distribution in a_μ^{HLO} with respect to the samples. We pick 1000 different samples of

Label	L/a	β	am_π	$m_\pi L$	a [fm]	m_π [MeV]
A3	32	5.20	0.1893(6)	6.1	0.0792(26)	472
A4	32	5.20	0.1459(7)	4.7	0.0792(26)	364
A5	32	5.20	0.1265(8)	4.0	0.0792(26)	315
B6	48	5.20	0.1073(7)	5.2	0.0792(26)	267
E5	32	5.30	0.1458(3)	4.7	0.0631(21)	456
F6	48	5.30	0.1036(3)	5.0	0.0631(21)	324
F7	48	5.30	0.0885(3)	4.2	0.0631(21)	277
G8	64	5.30	0.0617(3)	3.9	0.0631(21)	193
N5	48	5.50	0.1086(2)	5.2	0.0499(19)	429
N6	48	5.50	0.0838(2)	4.0	0.0499(19)	331
O7	64	5.50	0.0660(1)	4.2	0.0499(19)	261

Table 1: The CLS ensembles used in this study. We use the determination of the scale via f_K [12] and the masses determined in [13].

30 and 40 data points, and the variation in a_μ^{HLO} is included in the systematic error estimate. The Q^2 dependence of the HVP is modelled by Padé approximants [4, 14],

$$\Pi_{1,2}^{\text{fit}}(Q^2) = \Pi(Q^2 = 0) - Q^2 \left(\frac{a_1}{b_1 + Q^2} + \frac{a_2}{b_2 + Q^2} \right), \quad (2.1)$$

$$\Pi_{2,2}^{\text{fit}}(Q^2) = \Pi(Q^2 = 0) - Q^2 \left(a_0 + \frac{a_1}{b_1 + Q^2} + \frac{a_2}{b_2 + Q^2} \right), \quad (2.2)$$

where we impose that $a_{1,2} > 0$ and $b_{1,2} > 0$, and $\Pi(Q^2 = 0)$ is determined via an extrapolation. This type of representation is known to converge to $\Pi(Q^2)$ [14]. We impose a conservative cut, $0 < a_\mu^{\text{HLO}} < 10^{-6}$, to avoid some isolated numerical instabilities in the fits. As an example we show our results on our most chiral ensemble G8 in figure 1, which has the largest statistical uncertainties. To determine the systematic error for a number of variations in the calculation, we use the extended frequentist method [15, 16]. For this procedure the central value is given through the median of the central values of all variations, and the central 68% of this distribution associated with the systematic error. The statistical error is computed by the median of each bootstrap sample for all variations. The statistical error is then given by the central 68% of the distribution of these medians. The analysis involves two steps, first a fit of the momentum dependence of the HVP for each ensemble and then an extrapolation of a_μ^{HLO} to the physical point. In the implementation of the extended frequentist method for the second step, we weight the distributions over the considered variations by the corresponding p -value of the fits.

3. Extrapolation of a_μ^{HLO} to the physical point

For the extrapolation to the physical point we fit the m_π^2 -dependence and lattice artifacts of

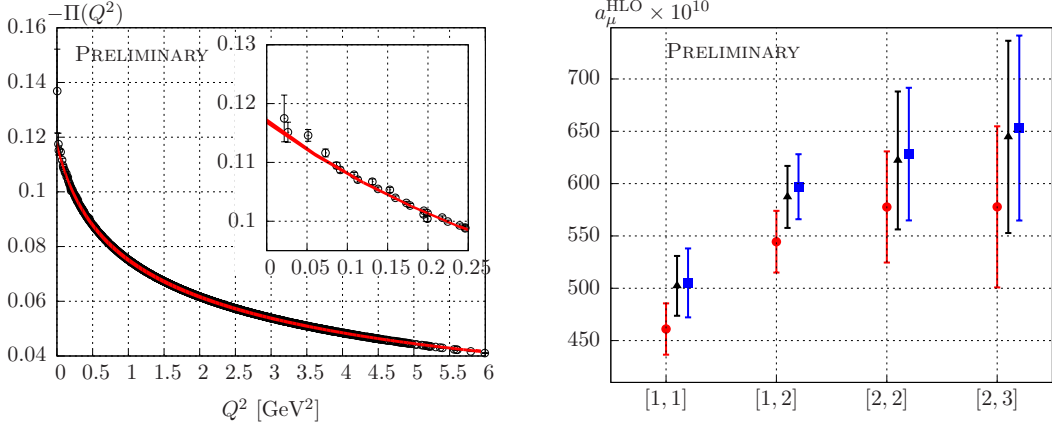


Figure 1: Left: The result for the HVP on G8, $m_\pi = 185$ MeV, $a = 0.0658$ fm, is shown in black. We combine the results determined via the extended frequentist method for the Padé [1,2], and a zoom into the small Q^2 region. We blow up the errors of the result in the plot of the full Q^2 range to make the curve visible. **Right:** We tested different orders of the Padé approximants for the fit functions and found that in fit interval used in this study the p -value of the fits with Padé order below [1,2] is low, while including [2,3] would only increase the error without adding new information.

$O(a)$ simultaneously using the following functions:

$$a_\mu^{\text{HLO,A}}(m_\pi^2, a) = c_1 + c_2 m_\pi^2 + c_3 m_\pi^2 \log(m_\pi^2) + c_4 a, \quad (3.1)$$

$$a_\mu^{\text{HLO,B}}(m_\pi^2, a) = c_1 + c_2 m_\pi^2 + c_3 m_\pi^4 + c_4 a, \quad (3.2)$$

where the fit ansatz $a_\mu^{\text{HLO,A}}(m_\pi^2, a)$ is inspired by chiral perturbation theory, and $a_\mu^{\text{HLO,B}}(m_\pi^2, a)$ is based on a more naive expansion in m_π^2 . Following [17] we also consider a linear function, i.e.

$$a_\mu^{\text{HLO,C}}(m_\pi^2, a) = c_1 + c_2 m_\pi^2 + c_3 a, \quad (3.3)$$

after rescaling the convolution function $w(r)$ in eq. (1.3) according to

$$w\left(\frac{Q^2}{m_\mu^2}\right) \longrightarrow w\left(\frac{Q^2}{m_\mu^2} \left(\frac{M_\rho^{\text{phys}}}{M_V}\right)^2\right). \quad (3.4)$$

Here M_V is the vector meson mass extracted from the vector correlation function, and the additional physical input from the experimental ρ -meson mass, M_ρ^{phys} , is inserted. The rescaling in eq. (3.4) provides an alternative for the chiral extrapolation and results in a milder pion mass dependence for a_μ^{HLO} . For every fit function we consider cuts on the contributing ensembles to the fit. For the fit functions of type $a_\mu^{\text{HLO,A}}(m_\pi^2, a)$ and $a_\mu^{\text{HLO,B}}(m_\pi^2, a)$ we first consider all ensembles and also impose cuts at $m_\pi < 400$ MeV and $a < 0.070$ fm. When $a < 0.070$ fm is used we switch off the term describing lattice artifacts, i.e. we set $c_4 = 0$, as we do not observe a clear lattice spacing dependence for the data, see e.g. figure 2. For the third ansatz, $a_\mu^{\text{HLO,C}}(m_\pi^2, a)$, we consider all ensembles and the cut $m_\pi < 400$ MeV. To illustrate the method we show the result we obtain for the fit function $a_\mu^{\text{HLO,A}}$ on the left of figure 2, where we evaluated the fit function in the continuum limit, which explains the vertical shift of the function with respect to the data.

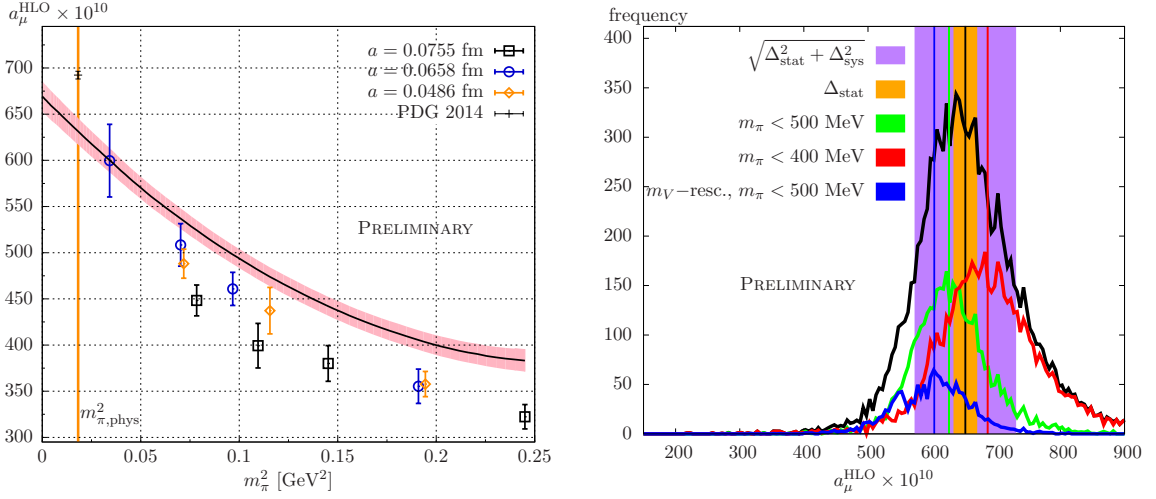


Figure 2: Left: Example of an extrapolation to the physical point with $a_\mu^{\text{HLO,A}}(m_\pi^2, a)$ using all ensembles for uds_Qc_Q . The fit function is evaluated in the continuum and thus appears above the data. The result from phenomenology is included as a reference. Right: The histogram derived from all possible variations (black). The statistical error is the orange band centered around the median shown in black of this histogram. The purple band includes the total error. To study the different systematic effects we project out different variations and build histograms with these projections of the data, the medians are shown as vertical lines in the corresponding color for each projection, respectively. We show the projections used to determine the contribution to the systematic error due to the chiral extrapolation.

To study the dominant of systematic effects projections of all variations used for the histogram are shown in black on the left of figure 2. For each projection we compute the median, and the standard deviation of these medians gives a rough estimate for the contribution to the total systematic error. To illustrate we show the projections for the effect of the chiral extrapolation in red, blue, and green in the same figure. We have one subgroup for the extrapolations based on $a_\mu^{\text{HLO,}\{A,B,C\}}(m_\pi^2, a)$ using all ensembles, and one subgroup for the fit functions $a_\mu^{\text{HLO,}\{A,B\}}(m_\pi^2, a)$ with the cut $m_\pi < 400$ MeV. The third subgroup consists of the results obtained using $a_\mu^{\text{HLO,C}}(m_\pi^2, a)$. To probe the contribution due to lattice artifacts we use two subgroups. The first subgroup consists of the fit functions $a_\mu^{\text{HLO,}\{A,B,C\}}(m_\pi^2, a)$ where we use a term proportional to lattice artifacts, i.e. $c_4 \neq 0$ and $c_3 \neq 0$, respectively. The second consists of the fits where we set $c_4 = 0$ using only $a_\mu^{\text{HLO,}\{A,B\}}(m_\pi^2, a)$. Other sources of systematic error include the choice of Padé approximant used to fit the HVP, as well as the picking of samples of subsets of data points, in order to perform viable correlated fits. We show the normalized results for the different contributions to the systematic error in table 2. We find that the uncertainty due to the chiral extrapolation dominates. The systematic effects introduced due to picking samples of the HVP data is also a sizeable contribution. Lattice artifacts and the choice of Padé approximant for the fit to the HVP are of the same order, while the number of points per Q^2 -sample appears to be negligible.

In figure 3 we compare our preliminary results, shown in blue, to other lattice groups sorted by valence quark contributions. The inner error bars show the statistical error only, while the outer error bars include the systematic errors summed in quadrature. The uncertainty on our preliminary results is dominated by a conservative estimate of the systematic effects.

Label	ud	uds_Q	$uds_Q c_Q$
χ -extrapolation	47%	42%	40%
Lattice artifacts	10%	14%	15%
Q^2 -sampling	31%	31%	34%
Padé	11%	12%	11%
Points/ Q^2 -sample	<1%	<1%	<1%

Table 2: We list the relative contribution of the sources of the systematic error for each flavor combination separately.

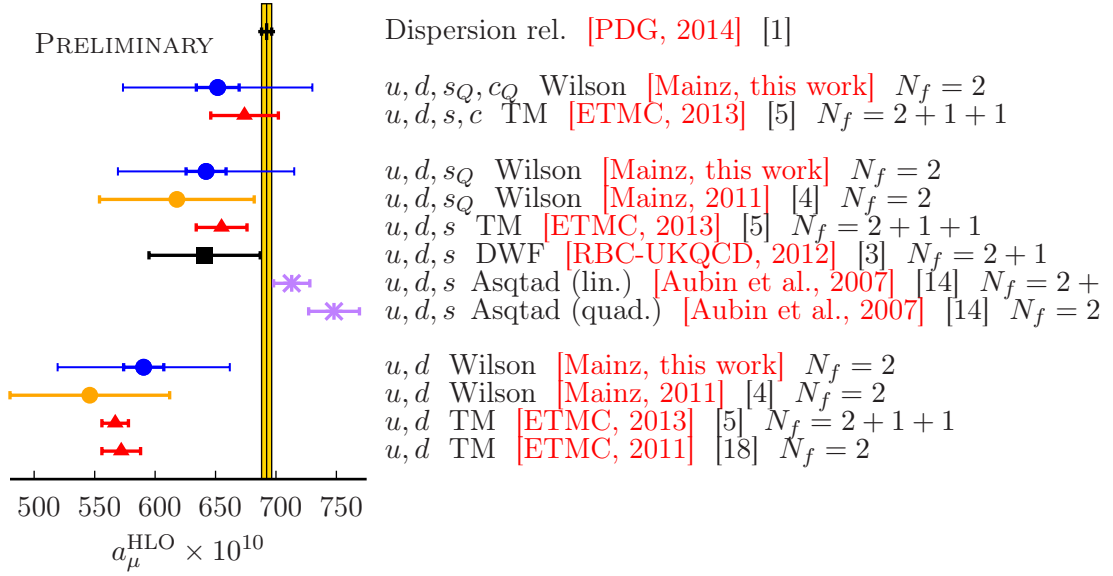


Figure 3: We show our updated results in blue for a_μ^{HLO} in comparison to the results of various groups sorted by valence quark contribution. The inner error bar on the blue points is the statistical error only, the outer error bar includes systematic errors summed in quadrature.

4. Conclusions and outlook

We have presented an implementation of an extended frequentist method to estimate the systematic uncertainties in the determination of a_μ^{HLO} . We consider a large number of variations including cuts on the set of available ensembles and various fit ansätze to describe the momentum dependence, lattice artifacts and the pion mass dependence. In order to deal with the large statistical correlations among Q^2 -points, we generate stochastic samples consisting of 30 and 40 points only. Our conservative estimate of the systematic errors dominates the overall uncertainty of our preliminary results.

We are currently investigating various approaches to improve the accuracy of our determination of a_μ^{HLO} . These include a dedicated study of the low Q^2 regime [19] in combination with the use of time moments [20]. Furthermore, we are also investigating the mixed-representation method [21], as well as using the Adler function to compute a_μ^{HLO} [22].

ACKNOWLEDGEMENTS: Our calculations were performed on the “Wilson” and “Clover” HPC Clusters at the Institute for Nuclear Physics, University of Mainz. We thank Dalibor Djukanovic and Christian Seiwerth for technical support. This research has been supported in part by the DFG via the SFB 1044. G.H. acknowledges support by the the Spanish MINECO through the Ramón y Cajal Programme and through the project FPA2012-31686 and by the Centro de excelencia Severo Ochoa Program SEV-2012-0249. This work was granted access to the HPC resources of the Gauss Center for Supercomputing at Forschungszentrum Jülich, Germany, made available within the Distributed European Computing Initiative by the PRACE-2IP, receiving funding from the European Community’s Seventh Framework Programme (FP7/2007-2013) under grant agreement RI-283493 (project PRA039) and ERC grant agreement No 279757.

References

- [1] K. A. Olive *et al.* [Particle Data Group Collaboration], *Chin. Phys. C* **38** (2014) 090001.
- [2] C. Aubin and T. Blum, *Phys. Rev. D* **75** (2007) 114502, hep-lat/0608011.
- [3] P. Boyle, L. Del Debbio, E. Kerrane and J. Zanotti, *Phys. Rev. D* **85** (2012) 074504, arXiv:1107.1497.
- [4] M. Della Morte, B. Jäger, A. Jüttner and H. Wittig, *JHEP* **1203** (2012) 055, arXiv:1112.2894.
- [5] F. Burger *et al.* [ETM Collaboration], *JHEP* **1402** (2014) 099, arXiv:1308.4327.
- [6] M. Della Morte *et al.*, *JHEP* **0507** (2005) 007, hep-lat/0505026
- [7] E. de Rafael, *Phys. Lett. B* **322** (1994) 239, hep-ph/9311316.
- [8] T. Blum, *Phys. Rev. Lett.* **91** (2003) 052001, hep-lat/0212018.
- [9] C. T. Sachrajda and G. Villadoro, *Phys. Lett. B* **609** (2005) 73, hep-lat/0411033.
- [10] P. F. Bedaque and J. -W. Chen, *Phys. Lett. B* **616** (2005) 208, hep-lat/0412023.
- [11] G. M. de Divitiis, R. Petronzio and N. Tantalo, *Phys. Lett. B* **595** (2004) 408, hep-lat/0405002.
- [12] P. Fritzscht *et al.*, *Nucl. Phys. B* **865** (2012) 397, arXiv:1205.5380.
- [13] S. Capitani *et al.*, *Phys. Rev. D* **92** (2015) 5, 054511, arXiv:1504.04628.
- [14] C. Aubin, T. Blum, M. Golterman and S. Peris, *Phys. Rev. D* **86** (2012) 054509, arXiv:1205.3695.
- [15] W-M Yao et al 2006 *J. Phys. G: Nucl. Part. Phys.* **33** 1
- [16] S. Durr *et al.*, *Science* **322** (2008) 1224, arXiv:0906.3599.
- [17] D. B. Renner *et al.*, *PoS LATTICE 2011* (2012) 022, arXiv:1206.3113.
- [18] X. Feng *et al.*, *Phys. Rev. Lett.* **107** (2011) 081802, arXiv:1103.4818.
- [19] M. Golterman, K. Maltman and S. Peris, *Phys. Rev. D* **90** (2014) 7, 074508, arXiv:1405.2389.
- [20] B. Chakraborty *et al.*, *PoS LATTICE 2013* (2014) 309, arXiv:1401.0669.
- [21] A. Francis, B. Jäger, H. B. Meyer and H. Wittig, *Phys. Rev. D* **88** (2013) 054502, arXiv:1306.2532.
- [22] M. Della Morte *et al.*, *PoS LATTICE 2014* (2014) 162, arXiv:1411.1206.